

A CORRELATION BETWEEN LIGHT PROFILE AND [MG/FE] ABUNDANCE RATIO IN EARLY-TYPE GALAXIES

ALEXANDRE VAZDEKIS¹, IGNACIO TRUJILLO² AND YOSHIHIKO YAMADA³

¹ Instituto de Astrofísica de Canarias, E-38200 La Laguna, Tenerife, Spain; vazdekis@ll.iac.es

² Max-Planck-Institut für Astronomie, Königstuhl 17, D-69117 Heidelberg, Germany and

³ National Astronomical Observatory of Japan, 2-21-1 Osawa, Mitaka, Tokyo 181-8588, Japan

Draft version October 29, 2018

ABSTRACT

We explore possible correlations between light profile shapes, as parameterized by the Sérsic index n or the concentration index $C_{re}(1/3)$, and relevant stellar population parameters in early-type galaxies. Mean luminosity weighted ages, metallicities and abundance ratios were obtained from spectra of very high signal-to-noise and stellar population models that synthesize galaxy spectra at the resolution given by their velocity dispersions σ , in combination with an age indicator ($H\gamma_\sigma$) that is virtually free of the effects of metallicity. We do not find any significant correlation between n (or $C_{re}(1/3)$) and mean age or metallicity, but a strong positive correlation of the shape parameters with Mg/Fe abundance ratio. This dependence is as strong as the Mg/Fe – σ and $C_{re}(1/3)$ – σ relations. We speculate that early-type galaxies settle up their structure on time-scales in agreement with those imposed by their Mg/Fe ratios. This suggest that the global structure of larger galaxies, with larger Mg/Fe ratios and shorter time-scales, was already at place at high z , without experiencing a significant time evolution.

Subject headings: galaxies: abundances — galaxies: clusters: individual (Virgo) — galaxies: fundamental parameters — galaxies: photometry — galaxies: stellar content — galaxies: structure

1. INTRODUCTION

A successful galaxy formation model should be able to explain the main scaling relations followed by early-type (E/SO) galaxies. These galaxies show up a tight relation between the size (by means of the effective radius r_e), surface brightness, and central velocity dispersion, σ , which is known as the Fundamental Plane (Djorgovski & Davis 1987; Dressler et al. 1987). Early-type galaxies also follow the Color-Magnitude Relation, CMR, i.e. brighter galaxies look redder (Visvanathan & Sandage 1977; Bower et al. 1992). The CMR and the Mg₂– σ relation (e.g. Bender, Burstein & Faber 1992; Colless et al. 1999) links the mass of a galaxy, through its luminosity, to its constituent stellar populations. However, little is known about the relation between the morphological shape and the stellar populations of early-type galaxies (Conselice 2003), most likely because these two fields rely on methods that have been traditionally disconnected.

From a stellar population point of view, measured colors and absorption line-strengths are translated to mean ages and metallicities via stellar population synthesis models. Using these models the CMR is often interpreted as a metallicity sequence (e.g., Arimoto & Yoshii 1987), i.e. elliptical galaxies are old and passively evolving systems (e.g., Ellis et al. 1997; Stanford, Eisenhardt & Dickinson 1998). However, this view is questioned by some studies, which show evidence for a significant intermediate age population in some ellipticals (e.g., González 1993; Jørgensen 1999). Element ratios provide further constraints on the star formation histories (e.g. Worthey 1998). These studies have shown compelling evidence for a systematic departure from solar element ratios of some elements as a function of σ (Trager et al. 2000). Recent modeling efforts have predicted spectra of stellar populations at moderately high resolution (Vazdekis 1999; Schiavon et al. 2002; Bruzual & Charlot 2003), leading to more accurate stellar population parameter estimates (Vazdekis & Arimoto 1999; Vazdekis et al. 2001a; Kuntschner et al. 2002).

From the point of view of galaxy structure, the shape of the overall surface brightness as parametrized by Sérsic

(1968) index, n , correlates with the global properties of early-type galaxies: total luminosity, central surface brightness and effective radius, r_e (Graham, Trujillo & Caon 2001 and references therein). Nowadays it is clear that the above luminosity-dependent departures from de Vaucouleurs profile are real, as clearly proven by the existence of strong correlations between n (or equivalently galaxy central concentration of light $C_{re}(1/3)$) (Trujillo, Graham & Caon 2001)) and the photometric-independent properties, σ (Graham, Trujillo & Caon 2001) and galaxy’s supermassive black hole mass (Graham et al. 2001b).

Aiming at exploring possible correlations between galaxy light profiles and their stellar populations we combine in this letter the results obtained from applying these modeling developments to high quality spectroscopic data. We find a tight correlation between [Mg/Fe] ratio and the shape parameters.

2. GALAXY MEASUREMENTS

We use the results derived by Vazdekis et al (2001a) and Yamada et al. (2003a, in prep.) for the stellar populations of 14 early-type galaxies in the Virgo cluster. We also included here 7 early-type galaxies in lower density environments (Yamada et al. 2003b, in prep.). Long-slit spectra of extremely high quality were obtained at the William Herschel (4.2m) and the Subaru (8.2m) telescopes, covering the range $\lambda \sim 4000\text{--}5500 \text{ \AA}$, at resolution $2.0\text{--}3.1 \text{ \AA}$ (FWHM). Signal-to-noise ranges from 100 to 500 (S/N per \AA unit), with larger values for galaxies with larger σ ’s, to be able to accurately measure the new $H\gamma_\sigma$ age indicator of Vazdekis & Arimoto (1999). Spectra were flux calibrated and summed up within $r_e/10$. Line-strengths and σ were measured from the summed spectra. Note that half of the sample has $\sigma < 150 \text{ kms}^{-1}$, allowing us to cover a large galaxy mass range.

Mean luminosity weighted ages, metallicities and abundance ratios were estimated by comparing selected absorption line-strengths with those predicted by the model of Vazdekis (1999). This model provides flux calibrated spectra in the optical range at resolution 1.8 \AA (FWHM) for single burst stel-

TABLE 1. GALAXY MEASUREMENTS

NGC	n	Ref	$C_{re}(1/3)$	$\sigma(\text{km s}^{-1})$	Age (Gyr)	[M/H]	[Fe/H]	[Mg/H]	[Mg/Fe]
Virgo galaxies									
4239	0.67	2	0.17	82	$5.5^{+1.9}_{-1.7}$	$-0.21^{+0.11}_{-0.10}$	$-0.21^{+0.09}_{-0.09}$	$-0.16^{+0.15}_{-0.14}$	$0.05^{+0.10}_{-0.09}$
4339	3.50	1	0.44	142	$12.6^{+5.3}_{-2.8}$	$-0.06^{+0.10}_{-0.06}$	$-0.17^{+0.07}_{-0.07}$	$+0.13^{+0.15}_{-0.15}$	$0.30^{+0.11}_{-0.11}$
4365	6.08	1	0.55	245	$20.4^{+3.1}_{-6.4}$	$-0.02^{+0.10}_{-0.08}$	$-0.28^{+0.16}_{-0.08}$	$+0.21^{+0.21}_{-0.16}$	$0.49^{+0.08}_{-0.11}$
4387	1.92	1	0.34	105	$15.1^{+5.4}_{-4.8}$	$-0.20^{+0.11}_{-0.11}$	$-0.22^{+0.10}_{-0.08}$	$-0.09^{+0.19}_{-0.10}$	$0.13^{+0.12}_{-0.05}$
4458	2.55	1	0.40	105	$16.6^{+3.9}_{-5.6}$	$-0.31^{+0.13}_{-0.05}$	$-0.40^{+0.05}_{-0.10}$	$-0.05^{+0.16}_{-0.07}$	$0.35^{+0.14}_{-0.03}$
4464	2.61	1	0.38	135	$21.0^{+2.3}_{-7.1}$	$-0.32^{+0.12}_{-0.06}$	$-0.40^{+0.09}_{-0.07}$	$-0.03^{+0.12}_{-0.13}$	$0.37^{+0.06}_{-0.09}$
4467	1.54	2	0.28	75	$16.0^{+5.2}_{-5.3}$	$-0.23^{+0.13}_{-0.12}$	$-0.35^{+0.13}_{-0.08}$	$-0.08^{+0.18}_{-0.13}$	$0.27^{+0.08}_{-0.08}$
4472	6.27	1	0.55	306	$10.4^{+5.5}_{-4.1}$	$0.07^{+0.17}_{-0.20}$	$-0.12^{+0.15}_{-0.23}$	$+0.46^{+0.16}_{-0.37}$	$0.58^{+0.04}_{-0.17}$
4473	5.29	1	0.52	180	$10.3^{+3.1}_{-2.1}$	$0.15^{+0.07}_{-0.11}$	$-0.06^{+0.06}_{-0.08}$	$+0.48^{+0.08}_{-0.16}$	$0.54^{+0.04}_{-0.10}$
4478	1.98	1	0.33	135	$10.0^{+2.7}_{-2.8}$	$0.04^{+0.15}_{-0.12}$	$-0.08^{+0.12}_{-0.06}$	$+0.23^{+0.14}_{-0.17}$	$0.31^{+0.05}_{-0.14}$
4489	2.50	4	0.37	73	$3.1^{+0.6}_{-0.8}$	$0.20^{+0.18}_{-0.16}$	$+0.20^{+0.15}_{-0.15}$	$+0.23^{+0.17}_{-0.21}$	$0.03^{+0.06}_{-0.10}$
4551	1.89	1	0.32	105	$7.2^{+1.5}_{-0.9}$	$0.19^{+0.07}_{-0.09}$	$+0.07^{+0.05}_{-0.10}$	$+0.41^{+0.07}_{-0.12}$	$0.34^{+0.05}_{-0.05}$
4621	6.14	1	0.55	230	$10.3^{+2.4}_{-1.8}$	$0.26^{+0.08}_{-0.08}$	$-0.04^{+0.04}_{-0.04}$	$+0.64^{+0.05}_{-0.14}$	$0.60^{+0.02}_{-0.11}$
4697	3.70	3	0.45	168	$11.3^{+4.5}_{-2.7}$	$0.06^{+0.10}_{-0.11}$	$-0.10^{+0.06}_{-0.10}$	$+0.30^{+0.08}_{-0.17}$	$0.40^{+0.04}_{-0.09}$
Field galaxies									
584	4.70	2	0.50	217	$8.6^{+1.9}_{-2.3}$	-	$-0.03^{+0.04}_{-0.08}$	$+0.31^{+0.06}_{-0.10}$	$+0.34^{+0.07}_{-0.05}$
720	4.96	3	0.51	247	$10.9^{+7.0}_{-2.7}$	-	$-0.16^{+0.08}_{-0.08}$	$+0.58^{+0.12}_{-0.19}$	$+0.74^{+0.07}_{-0.14}$
821	4.00	2	0.47	199	$12.3^{+12.5}_{-5.6}$	-	$-0.15^{+0.17}_{-0.17}$	$+0.26^{+0.18}_{-0.23}$	$+0.41^{+0.04}_{-0.08}$
1700	5.99	2	0.54	233	$6.4^{+3.1}_{-1.7}$	-	$+0.04^{+0.08}_{-0.09}$	$+0.37^{+0.09}_{-0.15}$	$+0.34^{+0.09}_{-0.09}$
3379	4.64	3	0.49	201	$17.8^{+7.4}_{-6.9}$	-	$-0.29^{+0.08}_{-0.10}$	$+0.19^{+0.19}_{-0.10}$	$+0.48^{+0.12}_{-0.03}$
5831	4.72	3	0.50	166	$5.9^{+3.5}_{-1.9}$	$0.32^{+0.15}_{-0.13}$	$+0.14^{+0.15}_{-0.16}$	$+0.56^{+0.06}_{-0.18}$	$+0.42^{+0.04}_{-0.10}$
7454	2.55	4	0.38	112	$6.5^{+3.3}_{-1.8}$	-	$-0.20^{+0.09}_{-0.10}$	$-0.07^{+0.13}_{-0.14}$	$+0.13^{+0.06}_{-0.06}$

NOTE. — The numbers in column 3 indicate the n parameter sources: 1 Caon, Capaccioli & D’Onofrio (1993). 2 HST F555W archive images. 3 Fits to the profiles of Peletier et al. (1990). 4 V-band images from J. Blakeslee (private communication).

lar populations (SSPs). An important advantage over previous approaches, which only predicted the strengths of a number of absorption lines (e.g. Worthey 1994; Vazdekis et al. 1996), is that we are able to analyze galaxy spectra at the resolution given by their internal velocity broadening and instrumental resolution. Therefore we do not work at the resolutions ($\text{FWHM} > 8\text{\AA}$) of the Lick/IDS system (Worthey 1994), and we do not transform our line-strengths (directly measured on the flux-calibrated observational and synthetic spectra) to the response curve of the IDS spectrograph.

Plots of the strengths of several metal line indices such as Mgb (Worthey 1994) or Fe3 (Kuntschner 2000) versus $\text{H}\gamma_{\sigma}$, which is virtually free from metallicity dependence, provide almost orthogonal model grids, allowing us to accurately estimate galaxy mean ages as well as the abundances of these elements. For a given galaxy all these plots provide almost identical ages, but the obtained metallicities will be different if the galaxy shows a departure from scaled-solar element ratios as in the models. Since the Mgb index is by far dominated by Mg and the Fe3 index by Fe (Tripicco & Bell 1995), the obtained metallicities can be approximated to $[\text{Mg}/\text{H}]$ and $[\text{Fe}/\text{H}]$ abundances, respectively. These values are then used to estimate the $[\text{Mg}/\text{Fe}]$ abundance ratio. An extrapolation of the model grids is usually required to obtain the $[\text{Mg}/\text{H}]$ for most massive galaxies, which show the largest $[\text{Mg}/\text{Fe}]$ ratios, since the models only extend to $[\text{M}/\text{H}] = +0.2$. Finally, plotting the $[\text{Mg}/\text{Fe}]$ index (González 1993), which is nearly insensitive to non solar abundance ratios (Vazdekis et al. 2001a; Thomas, Maraston & Bender 2003), versus $\text{H}\gamma_{\sigma}$ allows us to derive the total metallicity $[\text{M}/\text{H}]$. An alternative approach for obtain-

ing the $[\text{Mg}/\text{Fe}]$ ratios can be followed using models specifically computed for different α -enhancements (e.g. Trager et al. 2000; Thomas et al. 2003), on the basis of the sensitivities of these lines to the abundance changes of the different species as tabulated in Tripicco & Bell (1995). It is worth noting that fitting galaxy spectra with single burst models provides mean luminosity-weighted ages and metallicities, which means that the presence of young populations dominate the mean age and therefore are easily detected. Table 1 summarizes our results.

The values of n for most of Virgo galaxies were taken from Caon, Capaccioli & D’Onofrio (1993) based on B-band profiles. For the remaining galaxies we proceeded as follows: *i*) Sérsic model fitting of published B-band profiles (Peletier et al. 1990) or *ii*) when B-band images were not available we fitted V or F555W HST light profiles derived from archive images (see footnote of Table 1). Due to the small B-V color gradient of early-type galaxies (e.g. Peletier et al. 1990), n does not depend much on the filter in use. For NGC 4239 and NGC 4489 a Sérsic law was unable to fit observed light profile and a bulge ($r^{1/n}$) plus disk (exponential) decomposition was applied and the derived n value corresponds to the bulge. An alternative way of describing the light profile shape is using the central concentration index of Trujillo et al. (2001), $C_{re}(1/3)$. This index, which has been shown to be robust against measurement errors (Graham et al. 2001a) and monotonically related to n , evaluates the fraction of light enclosed within $r_e/3$ divided by the light within r_e (i.e. half of the total light). We use both n and $C_{re}(1/3)$ indices. Errors for n have a typical uncertainty of 25% (Caon, Capaccioli & D’Onofrio 1993), which translates to 10–15% uncertainty in $C_{re}(1/3)$.

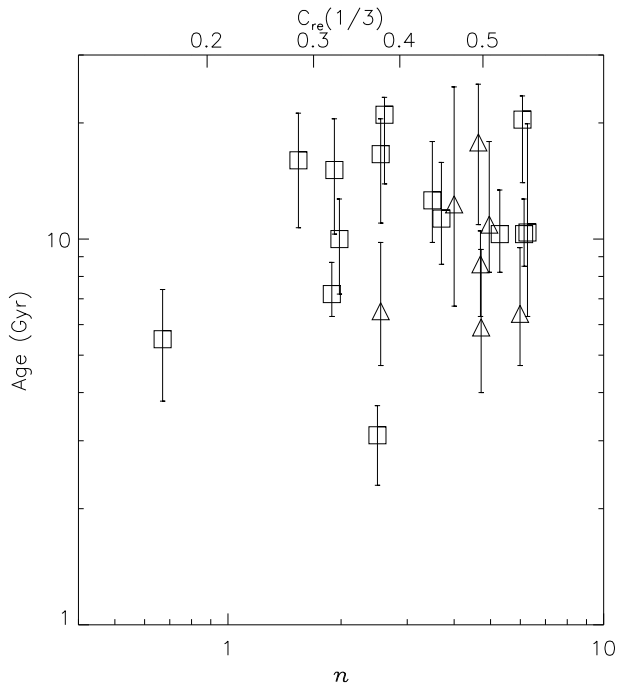


FIG. 1.— The shape parameters n and $C_{re}(1/3)$ versus mean luminosity weighted ages. Virgo galaxies are represented by open squares whereas field galaxies are represented by open triangles.

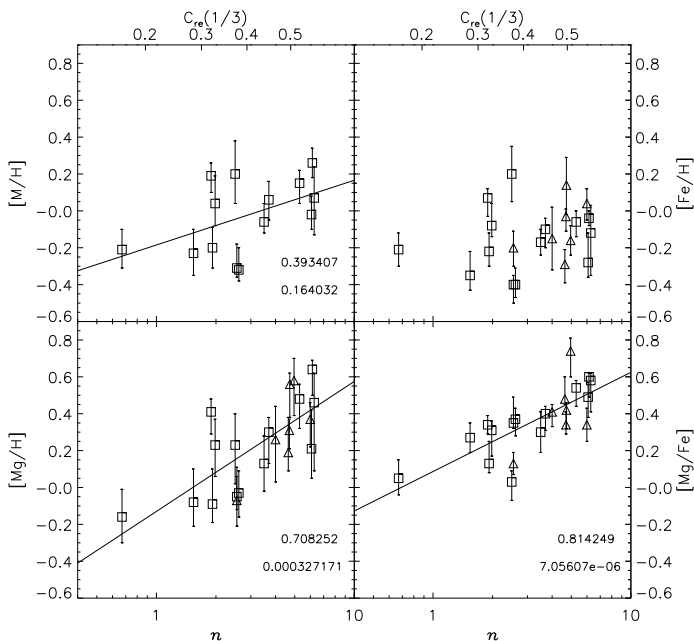


FIG. 2.— Shape parameters versus mean global metallicity [M/H], [Fe/H] and [Mg/H] metallicities and [Mg/Fe] abundance ratio. Symbols have same meaning as in Fig. 1. Spearman rank-order correlation coefficient and its significance value are written in each panel.

3. RESULTS

In this section we explore possible correlations between the shape and the stellar population parameters described in Section 2. In Fig. 1 we plot n and $C_{re}(1/3)$ indices versus mean luminosity weighted ages obtained for Virgo and field early-

type galaxies. We do not see a clear trend of the ages as a function of shape. It is worth noting that rather than absolute ages, which are subject of model uncertainties, we are interested in relative age trends (see Vazdekis et al. 2001b and Schiavon et al. 2002 for a detailed discussion on this issue).

We now focus on metallicities and abundance ratios. First panel of Fig. 2 shows the total metallicity [M/H] versus n and $C_{re}(1/3)$. Although we see that more metal-rich galaxies show higher $C_{re}(1/3)$ values the obtained correlation is weak, as shown by the Spearman test r_s . One would expect that larger galaxies with higher $C_{re}(1/3)$ (according to Graham, Trujillo & Caon 2001) and stronger potential wells would supply more fuel to their inner regions increasing their metallicity. This expectation might not be supported by our results.

Fig. 2 plots n and $C_{re}(1/3)$ versus Mg and Fe metallicities, showing no trend with Fe but a positive correlation with Mg. The latter can be understood if we combine the $C_{re}(1/3) - \sigma$ (Graham, Trujillo & Caon 2001) and $Mg_2 - \sigma$ (Bender et al. 1992; Colless et al. 1999) relations. No full agreement has yet been reached for the Fe - σ relation: Jørgensen (1999) finds that Fe abundance does not vary with σ , whilst Kuntschner (2000) finds a positive trend. This discrepancy can be in part attributed to the use or not of models including α -enhancement prescriptions (Thomas et al. 2003).

Fig. 2 shows for the first time a strong positive correlation between [Mg/Fe] abundance ratio and shape parameters. This is expected since [Mg/Fe] correlates with σ (Trager et al. 2000; Kuntschner 2000; Thomas, Maraston & Bender 2002), and σ correlates with $C_{re}(1/3)$ (Graham, Trujillo & Caon 2001). Nonetheless, it is surprising to see that [Mg/Fe] provides the strongest correlation among other relevant stellar population parameters, reaching a Spearman coefficient 0.8. A similar correlation strength is obtained by removing the galaxy with the smallest n value (i.e. NGC 4239).

4. DISCUSSION

To test how strong is the new correlation between the shape parameters and [Mg/Fe], we show in Fig. 3 the fits obtained for the already known $C_{re}(1/3) - \sigma$ and [Mg/Fe] - σ relations. We use the same galaxies plotted in Fig. 1 and Fig. 2. The [Mg/Fe] - n relation shows a correlation value as strong as the ones plotted in Fig. 3.

It is well known that early-type galaxies show non-solar abundance ratios (e.g., Trager et al. 2000). The [Mg/Fe] ratio, which spans a super-solar range (see Fig. 2), provides us with important clues on the star-formation time-scales. The α elements, such as Mg, are ejected to the ISM by SN II, which explode on short time-scales ($\leq 10^6 - 10^7$ yr). On the other hand, SN Ia are the main producers of Fe peak elements, which require time-scales around ~ 1 Gyr. It has been proposed that if the duration of the star formation is shorter than SN Ia time-scales the [Mg/Fe] should be larger than 0 (e.g., Worthey et al. 1992). Other possibilities have also been proposed, such as a top-heavy initial mass function (IMF), which could also be combined with a star formation that stopped before the products of SN Ia could be incorporated into the stars (e.g., Worthey et al. 1992; Vazdekis et al. 1996).

The fact that the central ($r_e/10$) σ and [Mg/Fe] measurements are strongly correlated (see lower panel of Fig. 3) suggests that the innermost regions of the more massive galaxies, with larger potential wells, stopped their star formation on shorter time-scales. Furthermore since the light concentration index strongly correlates with [Mg/Fe] suggests that early-type galaxies settled up their global (and not only

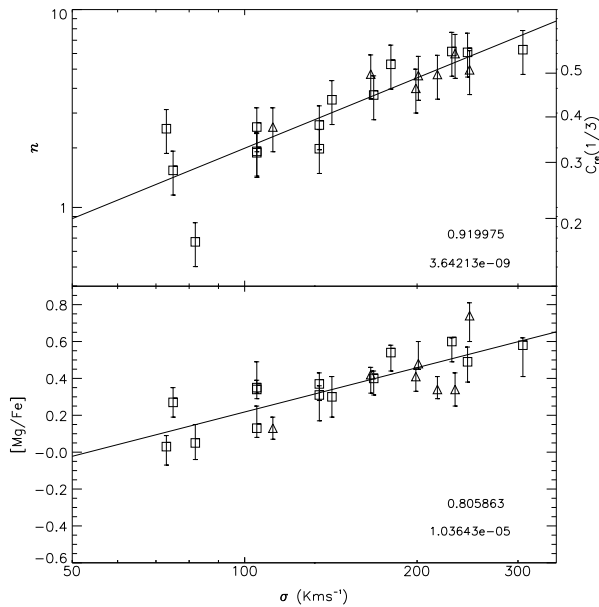


FIG. 3.— Galaxy velocity dispersion versus n and $C_{re}(1/3)$ and $[Mg/Fe]$. Symbols have same meaning as in Fig. 1

the innermost regions) structure on time-scales according to their $[Mg/Fe]$ ratios. This scenario would be reinforced if no $[Mg/Fe]$ radial gradients were present. Almost nothing is known about $[Mg/Fe]$ gradients outward galaxy effective radii, there are indications that this ratio is roughly constant at least out to $1 r_e$ (Halliday 1999; Mehlert et al. 2003). Mehlert et al. suggest that the constraint of short formation time-scales is a global feature and not only applies to galaxy centers.

We do not see a clear correlation between n and galaxy mean luminosity weighted ages but $[Mg/Fe]$ suggesting that the formation time-scale, rather than burst peppering as a function of time, is the main process linked to galaxy global structure. Since our galaxies are old and the time scales of

the larger galaxies very short, the new correlation suggests that the global structure of these galaxies was already at place at high z , without experiencing a significant time evolution. This result is supported by Chiosi & Carraro (2002) models, which suggest that the gravitational potential well (and therefore mass and shape of the galaxy) dictates the efficiency and extension of the star formation. The favoured picture is that early-type galaxies are assembled at high z (e.g., Fassano et al. 1998; van Dokkum & Ellis 2003), defining a tight sequence in the CM diagram at least out to $z \sim 1.2$ (Blakeslee et al. 2003), and their stellar populations evolve passively (e.g., Im et al. 2002; Schade et al. 1999). Furthermore, Mobasher et al. (2003) find that early-type galaxies show higher rest-frame B-band concentration indices than late-type spirals out to $z \sim 1$, which suggest that by that redshift value early-type systems have already developed large central light concentrations. Such high light concentrations are predicted by both the monolithic scenario by means of a rapid gas collapse which turns into stars, and within hierarchical galaxy formation framework via mergers of stellar and gaseous systems that take place at high z . Conselice (2003) shows that the light concentration is a key parameter to trace the past evolutionary history of galaxy formation.

This research will benefit from studies reaching deeper gradients of line-strengths and abundance ratios, and from theoretical efforts linking them to the light profiles (Angeletti & Giannone 2003). Including other element ratios in this analysis would provide further clues, since each element is expelled to the ISM at different epochs, and because line-strengths do not only depend on abundance but on other stellar population parameters. Sánchez-Blázquez et al. (2003) found that the CN is stronger in Virgo than in Coma galaxies. The near-IR CaII triplet, which is sensitive to both the Ca abundance and the IMF (Vazdekis et al. 2003), decreases as a function of σ (Saglia et al. 2002; Cenarro et al. 2003).

We thank N. Caon, H.-W. Rix and the referee for useful suggestions, and J. Blakeslee for providing us with photometric data for NGC 4489 and NGC 7454. Based on observations made with the European Southern Observatory telescopes obtained from the ESO/ST-ECF Science Archive Facility.

REFERENCES

- Angeletti, L., Giannone, P. 2003, *A&A*, 403, 449
Arimoto, N., & Yoshii, Y. 1987, *A&A*, 173, 23
Bender, R., Burstein, D., Faber, S.M. 1992, *ApJ*, 399, 462
Blakeslee, J.P. et al. 2003, *ApJ*, 596, L143
Bower, R.G., Lucey, J.R. & Ellis, R.S. 1992, *MNRAS*, 254, 601
Bruzual, G., Charlot, S., 2003, *MNRAS*, 344, 1000
Caon, N., Capaccioli, M. & D’Onofrio, M., 1993, *MNRAS*, 265, 1013
Cenarro, A.J., Gorgas, J., Vazdekis, A., Cardiel, N., Peletier, R. 2003, *MNRAS*, 339, L12
Chiosi, C., Carraro, G., 2002, *MNRAS*, 335, 335
Colless, M., Burstein, D., Davies, R.L., McMahan, R., Saglia, R. & Wegner, G. 1999, *MNRAS*, 303, 813
Conselice, C. 2003, *ApJS*, 147, 1
Djorgovski, S., Davis, M. 1987, *ApJ*, 313, 59
Dressler, A., Lynden-Bell, D., Burstein, D., Davies, R.L., Faber, S.M., Terlevich, R., Wegner, G. 1987, *ApJ*, 313, 42
Ellis, R.S., Smail, I., Dressler, A., Couch, W.J., Oemler, A.J., Butcher, H., Sharples, R.M., 1997, *ApJ*, 483, 582
Fasano, G., Cristiani, S., Arnouts, S., Filippi, M. 1998, *ApJ*, 115, 1400
González, J.J. 1993, Ph.D. thesis, Univ. of Lick, Santa Cruz
Graham, A., Trujillo, I., Caon, N. 2001, *AJ*, 122, 1707
Graham, A., Erwin, P., Caon, I., Trujillo, I. 2001, *ApJ*, 563, L11
Halliday, C. 1999, Ph.D. thesis, Univ. Durham
Im, M., et al. 2002, *ApJ*, 571, 136
Jørgensen, I. 1999, *MNRAS*, 306, 607
Kuntschner, H. 2000, *MNRAS*, 315, 184
Kuntschner, H., Smith, R., Colless, M., Davies, R. L., Kaldare, R., Vazdekis, A. 2002, *MNRAS*, 337, 172
Mehlert, D., Thomas, D., Saglia, R.P., Bender, R., Wegner, G. 2003, *A&A*, 407, 423
Mobasher, B., Jogee, S., Dahlen, T., De Mello, D., Conselice, C., Grogin, N., Livio, M. 2003, *ApJ Letters*, in press
Peletier, R. F., Davies, R. L., Illingworth, G. D., Davis, L. E., Cawson, M., 1990, *AJ*, 100, 1091
Saglia, R.P., Maraston, C., Thomas, D., Bender, R., Colless, M. 2002, *ApJ*, 579, L13
Sánchez-Blázquez, P., Gorgas, J., Cardiel, N., Cenarro, A.J., González, J.J. 2003, *ApJ*, 590, L91
Schade, D., et al. 1999, *ApJ*, 425, 31
Schiaivon, R., Faber, S., Rose, J.A., Castilho, B. 2002, *AJ*, 580, 873
Sérsic, J.-L. 1968, *Atlas de Galaxias Australes* (Cordoba: Obs. Astron.)
Stanford, S.A., Eisenhardt, P., Dickinson, M. 1998, *ApJ*, 492, 461
Thomas, D., Maraston, C., Bender, R. 2002, *Ap&SS*, 339, 897
Thomas, D., Maraston, C., Bender, R. 2003, *MNRAS*, 339, 897
Trager, S., Faber, S., Worthey, G., González, J. 2000, *AJ*, 120, 165
Tripicco, M., Bell, R.A. 1995, *AJ*, 110, 3035
Trujillo, I., Graham, A., Caon, N. 2001, *MNRAS*, 326, 869
van Dokkum, P., Ellis, R.S. 2003, *ApJ*, 592, L53

- Vazdekis, A. 1999, ApJ, 513, 224
Vazdekis, A., Cenarro, A.J., Gorgas, J., Cardiel, N., Peletier, R. 2003, MNRAS, 340, 1317
Vazdekis, A., Kuntschner, H., Davies, R.L., Arimoto, N., Nakamura, O., Peletier, R. 2001a, 551, L127
Vazdekis, A., Salaris, M., Arimoto, N., Rose, J. 2001b, ApJ, 549, 274
Vazdekis, A., Arimoto, N. 1999, ApJ, 525, 144
Vazdekis, A., Casuso, E., Peletier, R., Beckman, J. 1996, ApJS, 106, 307
Visvanathan, N. & Sandage, A. 1977, ApJ, 216, 214
Worthey, G. 1998, PASP, 110, 888
Worthey, G. 1994, ApJS, 95, 107
Worthey, G., Faber, S. M. & González, J. J., 1992, ApJ, 398, 69